

## Numerical simulation for the separation process of suspended fine sand from oil and water emulsion in a large-size sedimentation tank

Guoxi He<sup>a,\*</sup>, Siming Nie<sup>a</sup>, Liying Sun<sup>b</sup>, Dongliang Cao<sup>c</sup>, Kexi Liao<sup>d</sup>, Yongtu Liang<sup>a</sup>

<sup>a</sup>Beijing Key Laboratory of Urban Oil and Gas Distribution Technology, China University of Petroleum-Beijing, Beijing 102249, P.R. China, email: heguoxicup@163.com (G. He), 302732961@qq.com (S. Nie), liangyt21st@163.com (Y. Liang),

<sup>b</sup>SINOPEC Sales Company South China Branch, Guangzhou 510620, China, email: sunlyhe158@163.com (L. Sun)

<sup>c</sup>Changqing Oilfield Company the 9th Oil Production Plant, Yinchuan 750006, China, e mail: 891746837@qq.com (D. Cao)

<sup>d</sup>School of Petroleum Engineering, Southwest Petroleum University, Chengdu 610500, China, email: liaokxswpi@163.com (K. Liao)

Received 6 November 2017; Accepted 6 May 2018

### ABSTRACT

The high sand content of the crude oil produced from some oilfields influences the production efficiency. The fine sand deposits gradually in the three-phase separator during the treatment process of crude oil, which also seriously affects the dewatering treatment. To address the desanding and removal issue in high-sand-content oilfield, the large-size sedimentation tank is applied to enhance the treatment of the desanding process. Therefore, the numerical simulation for the separation process of suspended fine sand from oil and water emulsion in large-size sedimentation tank is implemented. The multiphase flow model of Eulerian and DPM model are chosen to simulate the depositing situation. The full flow field under different operating conditions for desanding is simulated and the applicable emulsion effluent standards under both static and dynamic sedimentation conditions are obtained. Comparing the simulated results to experimental results, a good agreement could be achieved. It was found that, the effluent-recycle process is not recommended if the viscosity-reduction process via heating is adopted to upgrade the desanding efficiency. The time required for desanding was 7–10 hours, and the volume of the large sedimentation tank which meets the current requirement was 3000 m<sup>3</sup>. The desanding efficiency can reach 90% when the sand size is larger than 80 μm, which provides guidance for whether to add the next level of desanding equipment or not. The formula for calculating the periodic time of cleaning deposited sand at tank bottom is given. It is also suggested that the sedimentation tank should be directly heated to reduce the liquid viscosity and prolong the sedimentation time, which is the optimum design for the whole desanding process.

**Keywords:** Suspended fine sand; High sand content emulsion; Large-size sedimentation tank; Desanding; Sand removal frequency

### 1. Introduction

There are a large number of loose sandstone oilfields in China, such as Shengli Oilfield and Gudong oilfield. The main problem in the production process of such fields is the high sand content in the crude oil [1–3]. The problem becomes more and more serious [4] due to the imperfect

production technology, unreasonable production rates, unsuitable production management, and so on. The desanding approach and corresponding technical process for sand removal must be added in the oil production system.

In 2000 and 2001, a follow-up observation on 3# sedimentation tank was conducted by high-sand-content oilfield, finding the sand was seriously accumulated at the bottom of the sedimentation tank. The deposition of sediment had also caused a blockage in the drainage hole, even

\*Corresponding author.

an overpressure in oil inlet and a blockage in the water effluent valve [5]. Sand deposition could reduce the effective volume of both separator and electric dehydrator, and move down the work efficiency. The sand deposition could also fray the equipment as well as lower the measurement precision of instrument. Additionally, it can do a great harm to the whole gathering and transportation system [6,7]. In a word, it is known that a lot of sand accumulates at the bottom of the sedimentation tank, thus, effective sand removal approach which adopted in sedimentation tank is urgent needed.

As the sand in crude oil could directly cause a dramatic increase in unpredictable consequences and the following economic costs [8,9], it is important to carry out the simulation of desanding process and the design of sand removal approach in the oilfield. At present, some high-sand-content oil fields have chosen the sedimentation tank to desand. However, the efficiency of the sedimentation tanks which is not in production yet remains unknown. How to select efficient sedimentation tanks is another outstanding subject. Therefore, it is of great significance to study the desanding efficiency of the sedimentation tanks in the CPF (central processing facility) [10].

Experiments [11] show that there are many different flow phenomena in the production system, such as density flow, stratified flow, condensation and subsidence, which makes the flow field very complicated. But in the sedimentation tank, the flow pattern is relatively simple. The method of studying the desanding effect of sedimentation tank is mainly concentrated on numerical simulation [12–17] due to the parameters of entire flow field in sedimentation tank can be obtained directly through numerical simulation.

Although reliable data could be provided, the experimental method is not often used in the study of oil-water-sand separation in the sedimentation tank especially in busy storage tank with large size because of the heavy workload and long experimental time, which is much longer than the actual allowable time. Therefore, it is very common to build a flow field based on fluid dynamics equations to simulate the sedimentation of solid impurities by gravity. Simulation can make up for the lack of experiments [18]. A two-phase model [5,10,12,13,19–22] based on fluid dynamics method is established to predict the distribution of phase velocity, track the trajectories of solid particles, and to simulate the effect of sedimentation tank structure on solid-liquid separation under different operating conditions. Thus, the design of sedimentation tank can be further optimized. Tanin [23] used CFD to evaluate the effect of extending the baffle in the inlet of a full-scale sedimentation tank (0.4 m\*0.4 m\*4 m) in order to improve sedimentation efficiency. Results showed that the baffle reduces the recirculation region in the entrance and accelerates the solid sedimentation velocity; finally, the solids sink downward to the bottom of the tank at a high speed. Considering the momentum exchange between water and solid, Tarpagkou and Pantokratoras [24] used DPM (discrete phase model) to study 3D hydrodynamics and the flow in the sedimentation tank (4 m\*6 m\*0.8 m). According to the results, as the size or components of dispersed phase increased, the effect that exerting on continuous fluid phase will also get stronger. Therefore, it is very important to carry out the simulation research on the sand content and the size distribution

of sand in the oil field gathering and transportation system. Guo et al. [25] studied the hydraulic behavior of a sedimentation tank (2.284 m\*2.701 m) using the finite element method. The sedimentation tank was equipped with adjustable baffles to better analyze particle settling. Results showed that the sedimentation tank mounting the adjustable baffle at 30° provided the best settling efficiency among the four different flow patterns. Patziger [26] has done a long-term research program on the improvement of existing shallow circular secondary settling tanks (SSTs) based on the computational fluid dynamics (CFD) investigation of their inner hydrodynamic processes and found a direct dependence between the inlet height and the length of the radial density jet induced by the entering water-sludge suspension. Bajcar et al. [27] investigated the influence of flow properties on a sedimentation process experimentally for two different types of circular settling tanks (about 0.89 m\*0.25 m\*0.2 m) with continuous operation. Research was focused on the influence of flow field on the sedimentation efficiency of both settling tanks. As can be seen, no large-size tank with volume of 3000 m<sup>3</sup> was studied before, and no sand cleaning frequency was introduced with sedimentation process. Additionally, the studies mentioned above were only focused on the field inside the tank and not intended to improve the desanding technology in the context of the whole process.

Through experiment, the physical properties of the crude oil in pipes are measured, and so as to the sand. The effects of the viscosity-temperature characteristics of the emulsion from the pipeline and crude oil are analyzed [28]. The size of the droplet and the sand are obtained. According to the numerical simulation on oil-water-sand flow field in sedimentation tank based on Fluent, the efficiency of desanding at different temperatures and the time of sand removal were measured, as well as the maximum diameter of sand and the sand content in processed oil, which can be used to optimize the desanding process to remove over 90% of the sand in the crude oil. The technical route of desanding research is shown in Fig. 1

The contribution of this work is that: (1) The simulations of full flow field under different operating conditions for desanding in large-size sedimentation tank are carried out. Comparing to the size of the studied tank in literature, the simulated one in this paper is quite larger. (2) The applicable emulsion effluent standards under both static and dynamic sedimentation condition are obtained, which could provide guidance for solid-liquid separation. (3) The calculation formula of periodic time for cleaning the deposited sand in tank bottom is given, which is not provided in previous studies. (4) Some experimental data of the diameters of water droplet and sand particle are obtained and the separation efficiency of sands with different sizes is concluded by tracing the sands' trajectory. (5) Optimal selection of large size tank for desanding and the detailed corresponding operating scheme could be achieved.

## 2. Mathematical model

### 2.1. Problem description and model assumptions

Crude oil in high-sand-content oilfield characterizes desanding demand, and generally there are no special sand

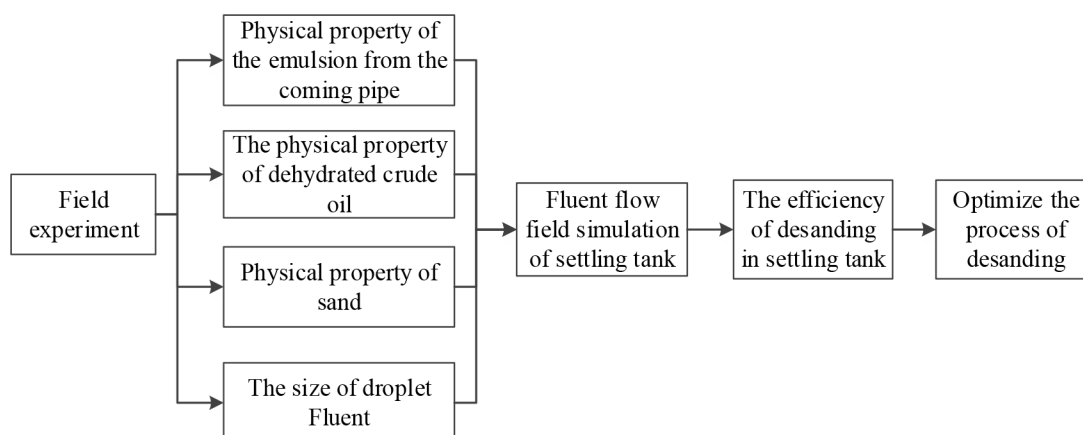


Fig. 1. The technical route of desanding research.

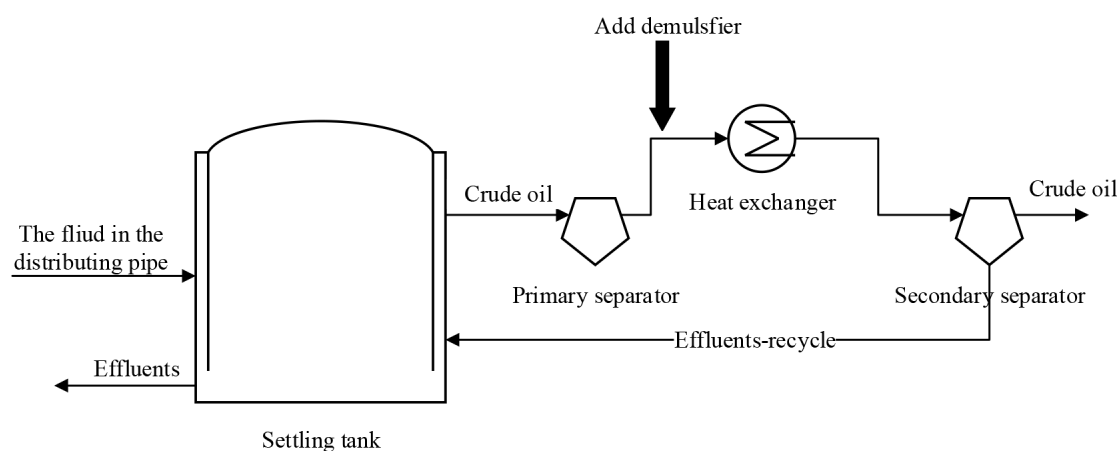


Fig. 2. The process after transformation.

removing device in CPF. The desanding process of crude oil is often completed by three-phase separator in processing station as shown in Fig. 2. The untreated oil directly moves into the primary separator so as to realize the preliminary separation of solid sand and liquid oil, free water and gas phase. After heating the oil-water emulsion in the heating stove, demulsifier is added into the secondary stage separator to further separate the combined water in the emulsion. Due to the low velocity of liquid in the three-phase separator (less than 0.05 m/s), the sediment has enough time to settle, which leads to a serious sand accumulation in the equipment and the sand further affects the dehydration of crude oil. In addition, the three-phase separator needs a regular cleaning (1–3 months). The total amount of the sediment can reach 90–120 mm in the primary and secondary separator. As the sand layer increases, the water content in three-phase separator is becoming higher and higher. What's more, the regular sand removal is a task of heavy workload and high cost. However, the work efficiency can be improved if the sand removing device is installed before the primary separator.

Thus, aiming to reduce the workload of regular sand removal and enhancing the efficiency of dehydration in the separator, the sand removal device is added before the crude oil entering the three-phase separator. The process of

crude oil dehydration after modification is shown in Fig. 2. The crude oil to be treated without heating is after the emulsion enters into the large tank for settling. After sedimentation, the crude oil containing less sand before entering the primary separator to further dehydrate. Then the demulsifier is added before the crude oil entering into the secondary separator.

In this paper, the numerical simulation will be carried out to testify the effect of improved technique of desanding and sand removal in sedimentation tank. It is also used to determine the running state of the sedimentation tank. The sedimentation tanks are used in many oilfields in China now as processing equipment, which combines oil-water separation, settlement and sand removal in the CPF. Fig. 3 is a structure illustration of sedimentation tank [29,30]. The sizes of the sedimentation tank in numerical model are given in Table 1.

After adding treating agent, crude oil (including oil, water, sand and other impurities) arrives at the inlet of the tank, and then reaches the bottom through the radial distribution pipes. After water washing, the free water, water with large size drops, salt and sand in the crude oil sink into the water layer. Because of gravity, the lighter oil will rise, while water and sand will sink, thereby separating the oil, water and sand.

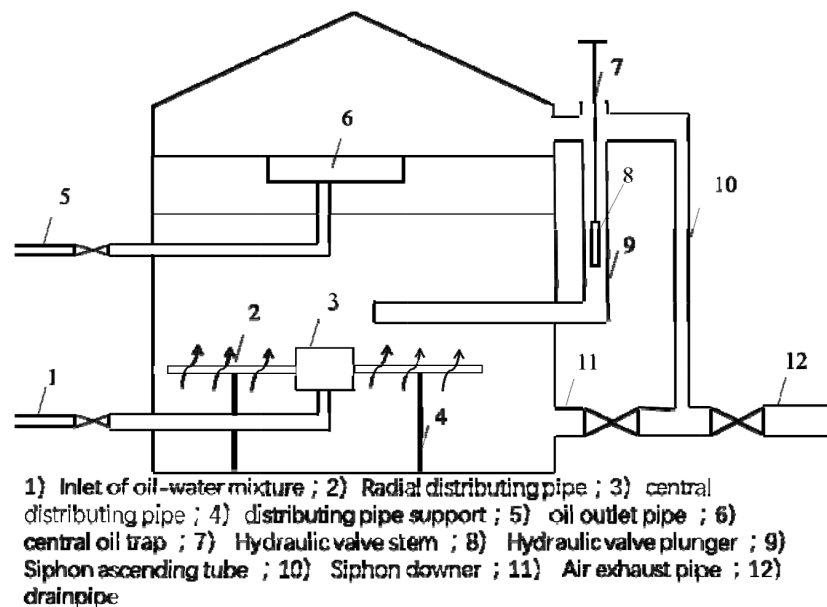


Fig. 3. The illustration of sedimentation tank structure in situ.

Table 1  
The sizes of the sedimentation tank in numerical model

Basic parameter	Dimension	Basic parameter	Dimension (shape)
Capacity of tank (m <sup>3</sup> )	3000	Diameter of tank (m)	18.00
Overall height of tank (m)	13.05	Diameter of inlet pipe (mm)	350
Tank wall height (m)	11.10	Diameter of oil outlet pipe (mm)	300
Distance between inlet and bottom (m)	0.80	Diameter of distributing pipe (mm)	300
Distance between oil pipe and bottom(m)	10.70	Diameter of distributing hole (mm)	100
Distance between outlet pipe and ground (m)	0.62	Number of distributing pipe	4
Distance between distributing pipe and bottom (m)	1.50	Number of distributing hole	5
Length of distributing pipe (m)	8.60	Shape of distributing hole	round

Because of the evident difference in density between sand and oil, water and oil-water emulsion, the sedimentation speed of the sand is obviously faster than that of water in oil-water separation. So the sand will firstly sink to the bottom of the tank. As time goes by, the sand at the bottom of the sedimentation tank accumulates, as a result, the sand cleaning is needed when it reaches a certain thickness. As shown in Fig. 3, a sand pipeline is laid in the tank. When the sand accumulates to some degree, the water will act on the sediment to effluent it into the grit chamber.

In order to reflect the internal flow field in sedimentation tank, the following methods are adopted in geometric model: (1) Considering the multiplicity and the complexity of influence factor and also the time about 100 h that we intend to experiment, the 2D flow region has been adopted to simulate the flow field in sedimentation tank due to its less computational task but no lower accuracy than 3D region. (2) Due to the symmetry of flow field and concentration field, and their little changes in the settlement process which is only affected by gravity, half of the tank is simulated so as to reduce the amount of computation. (3) The oil-water interface controller is not set due to the variety of

the interface's location. (4) Pure oil directly flows out from the oil outlet without considering the oil bath. (5) The sand outlet is not set during the process of simulation because of the periodicity of the sand cleaning.

In the premise of not affecting the separation effect of oil, water and sand, the simplified simulation conditions are: (1) During the settling process, the sedimentation tank should be heated evenly, the operating pressure in it is constant and steady (atmospheric pressure). (2) Distributing pipe is designed and paved symmetrically in order to make the internal velocity field and concentration field symmetric. (3) Regardless of the gas in the tank, only the separation between oil, water and sand is simulated. (4) Spherical sand is adopted by fluent.

## 2.2. Numerical model of the desanding process in sedimentation tank

### 2.2.1. Geometry model of sedimentation tank

Many factors can affect the oil-water-sand separation in the sedimentation tank, among which geometric factor

is the most important one. Therefore, to choose geometry models, such rules should be followed: (i) minimize the number of structure components to simplify the model; (ii) make the results conformed as close as possible to the actual results.

The distributing pipe is a commonly adopted structure in the sedimentation tank. The geometric size adopted in this paper is the vertical sedimentation tank which is often used in situ. Fig. 4 is a simplified model used to simulate the sedimentation tank.

The quality of mesh has a considerable influence on the accuracy and efficiency of simulating the flow field. The sedimentation tank mesh is shown in Fig. 5.

It is hard to simulate the large-size tank in full-scale, considering the complexity in establishing 3D model, which owns a diameter of 18 m, a depth of 13.05 m and some other parts. The large amount of control volumes which we have employed 503456 (595\*845) grid cells could lead to a long time of running the simulating software. At the same time, there is duration of about 100 h of sedimentation process that we intend to simulate, where the solving process is also time-consuming. Besides, the flow field is mainly affected by gravity and changes slowly during the settlement process. Therefore, the 2D simplified model with the acceptable simulation time is

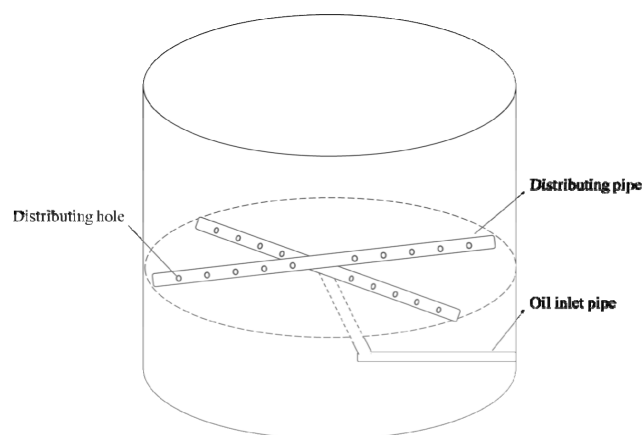


Fig. 4. The 3D model of the sedimentation tank.

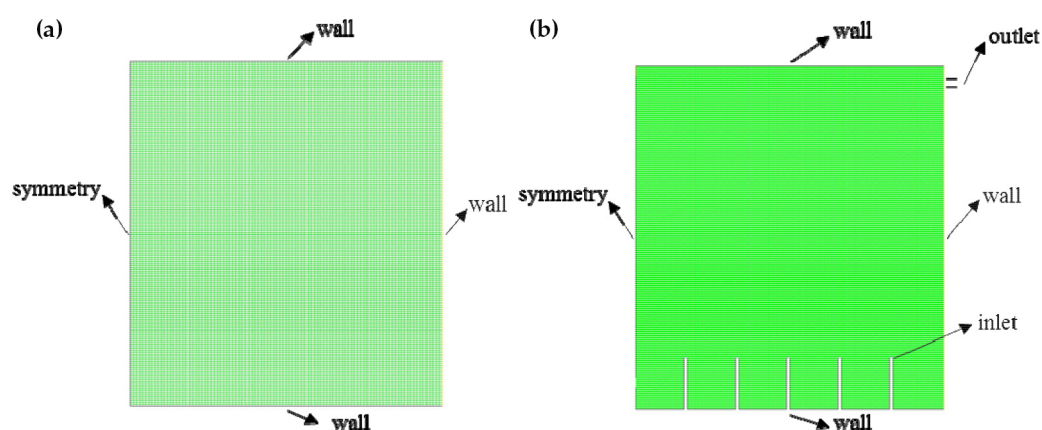


Fig. 5. 2D model of sedimentation tank (a) 2D model without distributing inlet (b) 2D model with distributing inlet.

employed to analyzing the process of separation and sedimentation. Table 2 shows the grid quality of sedimentation tank model.

This paper divides settlement tank simplified model about 117.45 m<sup>2</sup> area into 503,456 grids. Each grid occupies about 2.33×10<sup>-4</sup> m<sup>3</sup>, which is of high quality compared with 7.22×10<sup>-3</sup> m<sup>2</sup> in other paper [31].

### 2.2.2. Physical properties of emulsions, oil, water and sand

To conform to the actual situation in oilfield, the fluid adopted to simulate the flow field of oil-water separation is oil-water two-phase. The medium adopted in the analysis of emulsion-sand separation is emulsion and sand. Besides, the temperature in the tank is constant, and the physical properties of emulsion and sand are shown in Tables 2 and 3, respectively.

The viscosity-temperature data of produced liquid coming from flow line is shown in Table 3. Experimentally measured, the density of emulsion is 0.926 g/cm<sup>3</sup> and the water content in it is 44%.

The diameter distribution of water droplets in emulsion is shown in Fig. 6. Based on analysis, it can be found that the diameter of droplets in emulsion is in the range of 2–25 μm, and the size is smaller. The diameter within 10 μm makes the maximal proportion. Therefore, the emulsion mainly exhibits Newtonian in viscosity measurement. The droplet diameter parameter is required and currently used to define the properties of water droplet.

Table 2  
The grid quality of sedimentation tank model

Assessment parameter	Worst value	Standard
Aspect ratio	3.42	>1
Edge ratio	4.12	>1
Equi Angle skew	0.81	Between 0 and 1
Equi Size skew	0.78	Between 0 and 1
Size change	7.51	>0
Volume	1.22E-5	>0

Table 3  
The viscosity of fluid coming from pipe

Shear rate (1/s)	Viscosity (mPa·s)							
	26°C	30°C	35°C	40°C	45°C	50°C	55°C	60°C
50	160.2	140.3	120.0	104.0	91.0	80.2	70.3	58.0
60	158.9	141.2	121.1	104.2	90.4	78.8	69.4	58.2
70	159.7	140.8	120.3	103.8	90.0	79.5	70.0	58.0
80	159.0	141.4	120.8	102.9	91.3	78.6	69.5	56.9

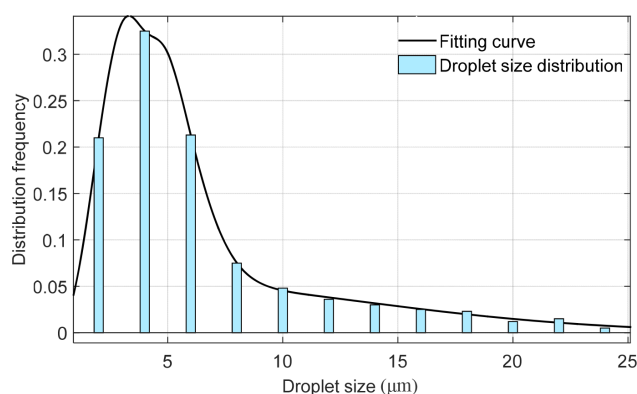


Fig. 6. Diameter distribution of water droplets in emulsion.

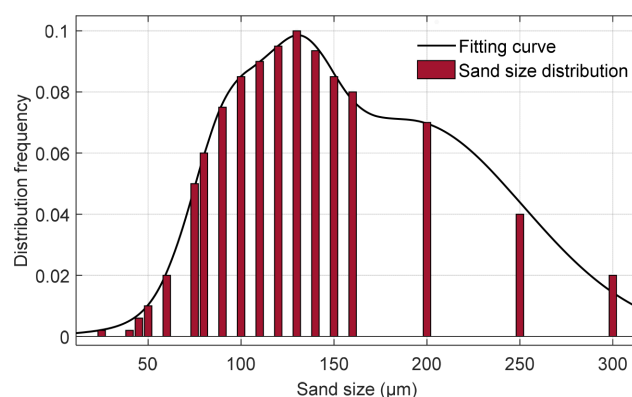


Fig. 7. The diameter distribution of sand in emulsion coming from pipe.

Fig. 7 shows the diameter distribution of sand is in the range of 40–300  $\mu\text{m}$  due to its larger density and diameter, the sand in oil sample could be removed during the process of sedimentation in some time.

The physical properties of the oil samples at the outlet of the secondary separator are tested. The test results are shown in Table 4. Relevant physical properties of fluid in the sedimentation tank are shown in Table 5.

The density of oil sample in secondary separator is  $0.886 \text{ g/cm}^3$ , the water content is 13%, and the salt content is  $99.6 \text{ mg/L}$ . No sand was detected in oil sample in secondary separator.

During the experiment, centrifugal is used to separate the sand and oil firstly, and then benzene is added to clean the separated sand. As a result, there is a small amount of sand loss in this process. It is estimated that sand cannot be detected when the sand content is less than 0.5% and the diameter of sand is less than 50  $\mu\text{m}$ .

The experimental data showed that the water content in oil sample is still 13% after the sedimentation in secondary separator, which means that the current process cannot meet the requirements of further dehydration of crude oil. Therefore, crude oil processing or process steps need to be improved. According to the test data of sand content, the process makes sense in sand removal, and most of the sand has been separated after the separation in the secondary separator.

### 2.2.3. Selection of theoretical models

Fluent software provides a large number of models, such as multiphase flow model, turbulence model, DPM (discrete phase model) and so on. To solving different problems, different models can be chosen to satisfy the accuracy

requirement of the simulation. Advantages and disadvantages of each multiphase flow model [24] are as follows. (1) VOF model. The volume fraction of each fluid is recorded in the whole flow unit. But the model is not suitable for the simulation of sand removal process. (2) Mixture model. This model can be used for a numerical simulation of two-phase or multiphase flow. The discrete phase is described by relative velocity in this model. Meanwhile, the mixture model can also be used for simulating the multiphase flow without discrete phase. What's more, the mixture model can be used to simulate oil-water-sand separation process. (3) Eulerian model. Eulerian model is the most complicated multiphase flow model in Fluent. It is generally used for floating, fluidized bed, particle suspension and so on. Its solution time needed is longer because of the larger computational work than that of the mixture model.

According to the best applicable conditions of each model, this study adopts the Eulerian model for oil and water two phases. The simulation of the oil-water two-phase flow field was first carried out to analyze the oil-water separation process. Then Eulerian model was also used to simulate the sand settlement process in sand-containing emulsions at different temperatures (viscosities) and different particle sizes.

The simulated inlet velocity is 1 m/s, and the inlet pipe diameter is 350 mm. So, the inlet Reynolds number is:

$$\text{Re} = \frac{vd}{\mu} = \frac{1 \times 350 \times 10^{-3}}{2.144 \times 10^{-6}} = 163246 \quad (1)$$

It is shown that the flow at the inlet of the sedimentation tank is turbulent flow, thus the turbulence model of RNG  $k-\epsilon$  [3] is selected.

Table 4  
Data of viscosity-temperature curve of dehydrated crude oil at outlet of secondary separator

Shear rate (1/s)	Viscosity (mPa·s)							
	26°C	30°C	35°C	40°C	45°C	50°C	55°C	60°C
50	58.8	51.0	43.0	36.5	31.1	26.4	22.1	17.7
60	57.2	50.3	43.0	36.2	31.1	26.3	22.1	17.5
70	58.1	51.0	42.6	36.2	31.0	26.7	22.1	17.3
80	57.8	50.5	42.8	36.7	30.3	26.5	22.0	17.2

Table 5  
Relevant physical properties of fluid in the sedimentation tank

Relevant property	Density (kg/m <sup>3</sup> )	Viscosity	Content
Water	988.0	According to experiment	44%
Crude oil	869.2	According to experiment	56%
Sand	2617.0	–	Set by relevant document

Thus, the governing equations include continuity, momentum, energy equations, and second order volume fraction equations, RNG  $k$ - $\varepsilon$  model equations [24–27].

(1) Continuity equation

$$\frac{\partial}{\partial t}(\rho_m) + \nabla \cdot (\rho_m \bar{v}_m) = \dot{m} \quad (2)$$

(2) Momentum equation

$$\frac{\partial}{\partial t}(\rho_m \bar{v}_m) + \nabla \cdot (\rho_m \bar{v}_m \bar{v}_m) = -\nabla p + \nabla \cdot [\mu_m (\nabla \bar{v}_m + \nabla \bar{v}_m^T)] + \rho_m \bar{g} + \bar{F} + \nabla \cdot \left( \sum_{k=1}^n V_k \rho_k \bar{v}_{dr,k} \bar{v}_{dr,k} \right) \quad (3)$$

(3) Energy equation

$$\frac{\partial}{\partial t} \sum_{k=1}^n (V_k \rho_k E_k) + \nabla \cdot \sum_{k=1}^n (V_k \bar{v}_k (\rho_k E_k + p)) = \nabla \cdot (k_{eff} \nabla T) + S_E \quad (4)$$

(4) Second phase volume fraction equation

$$\frac{\partial}{\partial t} (V_k \rho_k) + \nabla \cdot (V_k \rho_k \bar{v}_m) = -\nabla \cdot (V_k \rho_k \bar{v}_{dr,k}) \quad (5)$$

(5) RNG  $k$ - $\varepsilon$  model equation.

$$\frac{\partial}{\partial t} (\rho_m k) + \frac{\partial}{\partial x_j} (\rho_m u_{m,j} k) = \frac{\partial}{\partial x_j} \left( \frac{\mu_{eff,m}}{\sigma_k} \frac{\partial k}{\partial x_j} \right) + G_{m,k} - \rho_m \varepsilon \quad (6)$$

$$\frac{\partial}{\partial t} (\rho_m \varepsilon) + \frac{\partial}{\partial x_j} (\rho_m u_{m,j} \varepsilon) = \frac{\partial}{\partial x_j} \left( \frac{\mu_{eff,m}}{\sigma_\varepsilon} \frac{\partial \varepsilon}{\partial x_j} \right) + \frac{\varepsilon}{k} C_{1\varepsilon} G_{m,k} - C_{2\varepsilon} \rho_m \frac{\varepsilon^2}{k} \quad (7)$$

The formula for calculating the oil-water viscosity is as follows:

$$\frac{1}{\nu_m^3} = V_1 \nu_1^{\frac{1}{3}} + V_2 \nu_2^{\frac{1}{3}} \quad (8)$$

where  $\nu_1, \nu_2$  are the kinematic viscosity of oil and water respectively.  $V_1, V_2, V_3$  are the volume fraction of oil, water and sand, respectively, with no-dimensional form:  $V_1 + V_2 + V_3 = 1$ .

According to the characteristics of the multiphase flow model, if the volume fraction of one phase is less than 10%, it can be considered as the dispersed phase, where the DPM can be applied. Otherwise the available model is the Eulerian model. According to the optimum conditions of each model, the DPM model is used to simulate the trajectory of different sands with different sizes. The number of sand is  $N$ . The orbits of discrete phase particles were solved by integrating particles force differential equation in the Lagrangian coordinate system. Then the inlet particle concentration  $C_{sand}$  is calculated using the following formula

$$C_{sand} = \frac{\left( \sum_j^N Vol_j(d_p) \right)}{(Q \Delta t)} \quad (9)$$

The particle force balance equation in Cartesian coordinates ( $y$  direction) is [24,31]

$$\frac{du_p}{dt} = F_D (u - u_p) + \frac{g_y (\rho_p - \rho)}{\rho_p} + F_y \quad (10)$$

In the formula,  $F_D (u - u_p)$  is particle unit mass drag force.

$$F_D = \frac{18 \mu C_D Re}{\rho_p d_p^2 24} \quad (11)$$

In the formula:  $u$  is fluid phase velocity;  $u_p$  is particle velocity;  $\mu$  is fluid dynamic viscosity;  $\rho$  is fluid density;  $\rho_p$  is particle density;  $d_p$  is particle diameter;  $Re$  is relative Reynolds number (Granular Reynolds number), which is defined as

$$Re = \frac{\rho d_p |u_p - u|}{\mu} \quad (12)$$

The oil-water two-phase flow is firstly simulated. The oil-water separation process is analyzed. Then, the sand sedimentation process is simulated by implementation of Eulerian model, where the sand in emulsion has different particle size and the simulation is performed at different temperatures. Finally, the trajectories of sands with different sizes are tracked.

### 3. Results and discussion

To obtain a unique solution in simulated flow filed, both the initial conditions and the boundary conditions are defi-

nite solutions. A section of the inlet pipe of the sedimentation tank is used as an inlet, which served as the velocity-inlet boundary. Different entrance velocities are adopted for making comparison to find out suitable velocity-inlet range. If the velocity inlet range is not reasonable, there will be insufficient time for sand sedimentation and will lead to the primary separator removing sand frequently. The sand will be effluent with the emulsion thereby losing the effectiveness of the sedimentation tank. In addition, the turbulence specification method is introduced and the related parameters are as follows: the turbulence intensity is 3.56%, and the hydraulic radius is 0.353 m. According to the relevant conditions of oil-water outlet, as shown in Fig. 5, the oil-water outlet is chosen as the free outflow boundary. Therefore, the outlet has multiple outflow boundaries, and the mass flow-rate of oil-water outlet accounts for 80% and 20% of the total flow respectively. The default wall in Fluent, namely, the non-slip wall boundary condition is adopted. The turbulence velocity and fluid velocity on the wall are both zero. The symmetrical boundaries are used in symmetrical plane, which means both the flow flux and the heat flux are zero.

Before numerical simulation, it is necessary to give an initial value to the flow field, which is obtained by flow field initialization. Whether the initialization condition is correct or not has an important influence on the convergence speed and the accuracy of the calculation results.

### 3.1. Sand sedimentation simulation without injection

The process of oil-water separation and sand sedimentation at an inlet speed of 0 m/s is analyzed in this section. The comparisons of sand distribution after 7 h static separation and under different temperature conditions are also implemented.

#### 3.1.1. Oil-water separation simulation without emulsion injection

The 2D simplified model is employed to analyzing the process of separation and sedimentation, when considering the complexity in establishing 3D model and the solving process as well as the great similarity of the horizontal flow field in oil-water separation. The oil concentration of the emulsion is 80%. The concentration distribution of oil phase in different stages is obtained by simulation as Fig.8.

Although the oil and water have been uneven after 100 h sedimentation; the oil concentration in water phase is still relatively high, and needs longer time to separate. There is 7–8% of water at the top of the tank after 100 h sedimentation separation. At the bottom of the tank, the water increases only to 33.5%, which means although the water phase keeps depositing during the sedimentation process, the oil content is up to 66.5%. Therefore, it is difficult to separate oil and water without de-emulsifier.

#### 3.1.2. Oil-water-sand separation simulation without emulsion injection

Due to chemicals has been added into the emulsion before the two-stage separator, it is not reasonable to take

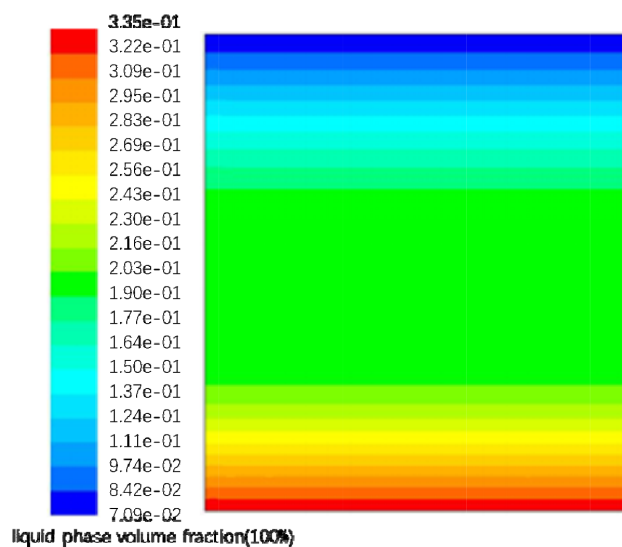


Fig. 8. The distribution of water and oil after 100 h sedimentation without emulsion injection (data is water volume fraction).

the oil-water separation criterion as constraint condition when setting simulation time in the tank. Therefore, the desanding effect by sedimentation is set as the constraint condition when carrying out the oil-water-sand separation simulation.

Fig. 9 shows the sedimentation process of sand without injection. The emulsion in the tank contains a sand content of 5%. Within 1 h, the sand content at the top 0.2 m range of the tank can be reduced to about 1%. With the increase of sedimentation time, the area range of sand content less than 1% is increasing gradually. The fluid height in which the sand content could meet the desanding standard has reached 1.5 m after 7 h, which is distinctly lower than the location of the oil collection pipe inlet. It means that the liquid at the top of the tank reaches the effluent standard. With the sand sedimentation downward gradually, the sand content at the bottom of the tank increases obviously. Considering the periodic sand removal in the sedimentation tank, the sand will deposit at a certain height at the bottom. Therefore, the position of the water outlet pipe shall be higher than the deposited sand height at the bottom of the tank.

Fig. 10 illustrates the comparison of sand distribution under the condition of 30°C and 50°C after 7 h static separation. By comparison, it can be found that the velocity of sand sedimentation is slow due to the high emulsion viscosity with 30°C. But the sand content of emulsion is less than 1% at about 1 m at the top of the tank, which still meets the requirements of desanding. Therefore, sand sedimentation after 7 h still meets the requirement without heating in the tank.

The distribution of sand velocity at different time is shown in Fig. 11. It is known that even if there is no injection, the sand cannot deposit in an ideal state of vertical velocity due to the influence of the wall as well as the interaction between sand particles, which means the velocity field has a vortex. The average velocity of sand subsidence decreases resulting in the increase of sedimentation time in comparison with the ideal calculation method of Stokes equation.

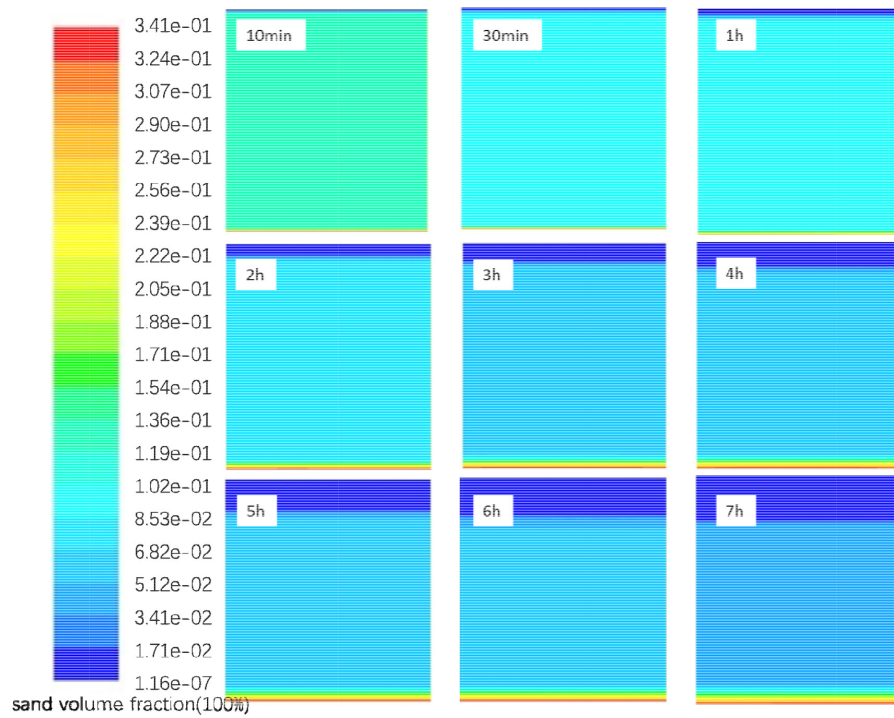


Fig. 9. The sand volume fraction during separation process without injection.

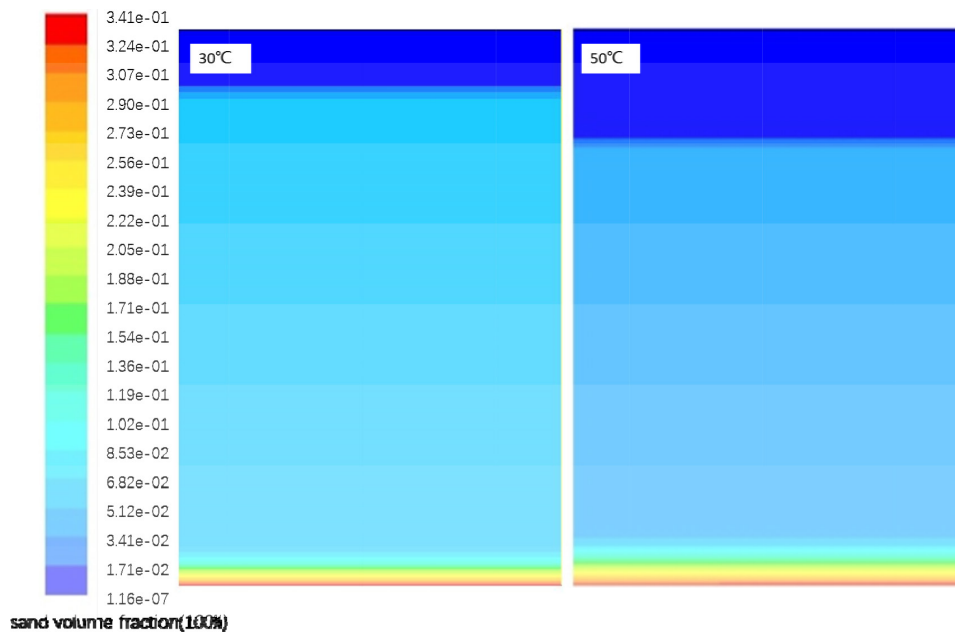


Fig. 10 The comparison of sand distribution during static separation process under 30°C and 50°C conditions.

Compared with the time of desanding, it can be concluded that the oil and water cannot be separated efficiently in sedimentation tank. If the produced liquid coming from the wells is the emulsion with high sand content, the primary task is desanding while the oil-water separation can be performed in the subsequent three-phase separator. Therefore, the sedimentation process of the sand in emulsion is mainly simulated in this paper.

### 3.2. Sand sedimentation simulation with injection

The emulsion containing sand flows into the sedimentation tank through the distributing pipe at a specified speed. The height of the distributing pipe outlet should be 1.5 m when inlet velocity exists. The high-sand-content oil field is located in Yumen oilfield in Gansu province, whose fluid production is about 3500–5400 m<sup>3</sup>/d. Then the inlet velocity

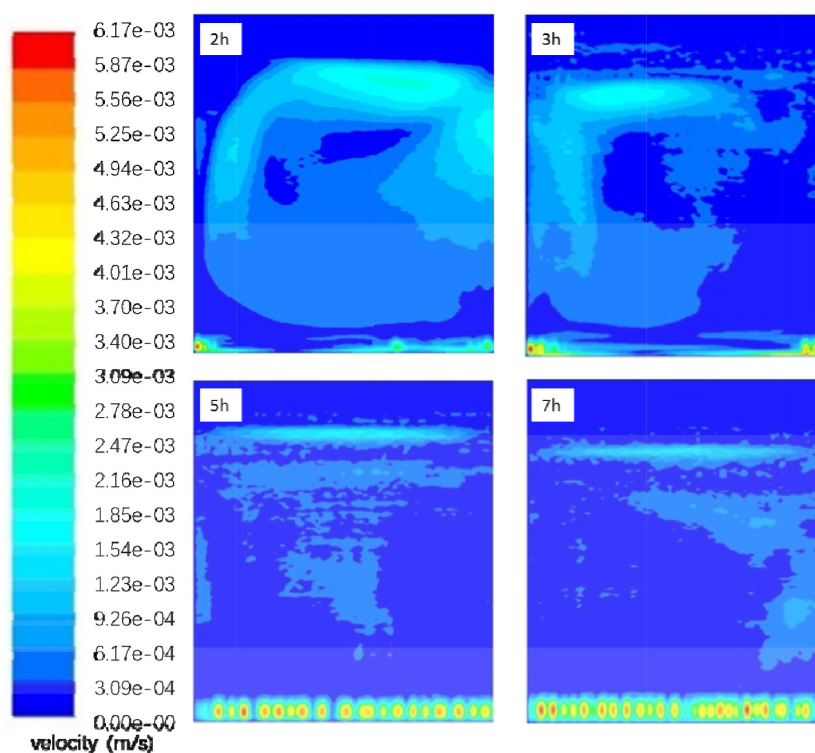


Fig. 11. The sand velocity field during the static separation process without injection.

at the distributing pipe can be calculated according to the fluid production and the tank capacity.

In the simulation model, it is assumed that the liquid phase is the continuous phase while the solid phase is the dispersed one. There is no sand but oil-water emulsion in the tank in the initial state. The emulsion with sand flows into the liquid distributor at a specified speed when the calculation begins. During this process, the total volume of fluid in the tank is stable in spite of the periodic sand removal operation. The water-in-oil emulsion can flow out freely from the oil collection pipe at the top of the tank while the water drainage is implemented through the drainpipe. Both of the hydrodynamic model of coupled solid-liquid phase flow and the energy equation are adopted, which indicates that the sand separation and sediment are in accordance with the turbulence model. The basic physical parameters of sand and the emulsion are mentioned above. Both of sand and the emulsion flow into the tank at a same velocity and with a fixed component proportion.

### 3.2.1. Effect of emulsion temperature on sand sedimentation

#### 3.2.1.1. Emulsion at 50°C with an injection speed of 0.01 m/s

The emulsion viscosity at inlet is 80 m Pa·s at 50°C. Figs. 12 and 13 show the distribution of liquid phase and solid phase in tank with 50°C and 0.01 m/s inlet, respectively. With the injection of emulsion with sand, the sand gradually deposits and assembles at the bottom of the tank. As the injection time prolongs, the concentration distribution of both of the sand and the emulsion gradually becomes stratified.

Fig. 14 illustrates the distribution of sand velocity. It can be seen that with the injection of emulsion, the sand gradually moves towards the top of the tank with a slow velocity, which indicates that some of the sands rise with the emulsion and move upwards for a period time. But most the sands gradually move down and accumulate at the bottom of the tank. Few sands in the emulsion reach the top of the tank after 5 h of injection, which means that the inlet speed of 0.01 m/s cannot meet the requirement of desanding in such specification of sedimentation tank.

The relation between the inlet flow rate  $v_{in}$  and the handling capacity of the sedimentation tank  $A$  is as follows:

$$A = nv_{in}t_1L_{in} \quad (13)$$

$$t_1 = \frac{A}{nv_{in}L_{in}} = \frac{V_{\text{tank}}}{Q_{in}} \quad (14)$$

Thus, the specification of the sedimentation tank which possesses appropriate capacity could be obtained.

#### 3.2.1.2. Emulsion at 40°C with an injection speed of 0.01 m/s

The viscosity of the emulsion at inlet is 104 m Pa·s at 40°C according to the experiment results. The concentration distribution of liquid and solid phase during dynamic separation process is shown in Figs. 15 and 16.

Due to the same inlet speed, the distribution of liquid and solid phase is similar to those at 50°C. By comparison, the different viscosities of liquid phase cannot lead to a distinctive difference in the concentration distribution of both emulsion and sand.

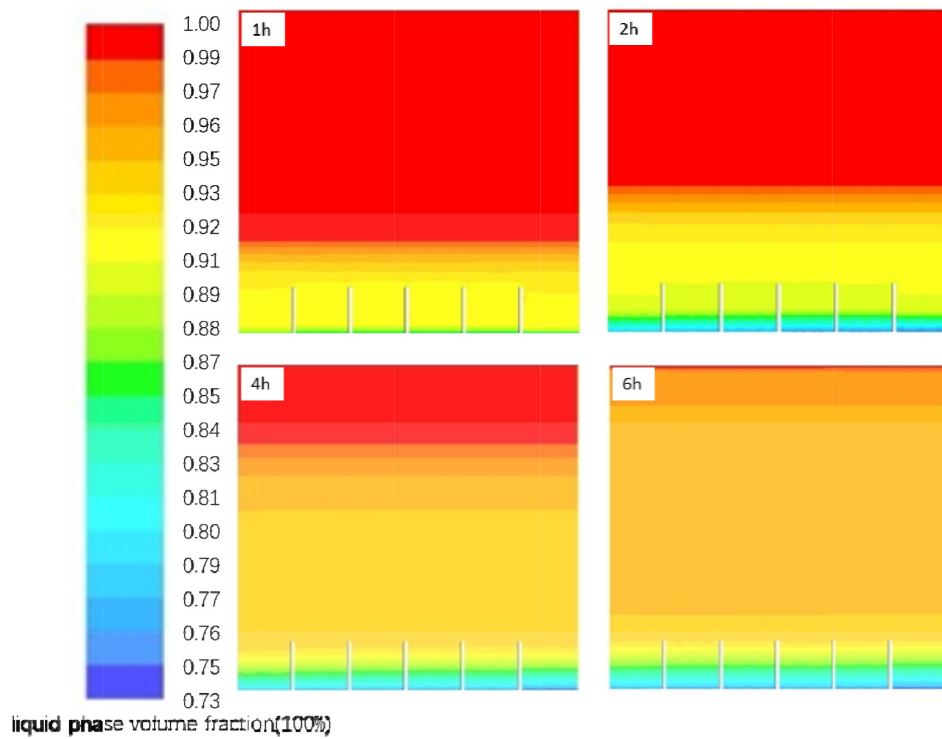


Fig. 12. The emulsion distribution during dynamic separation process at 50°C and 0.01 m/s inlet.

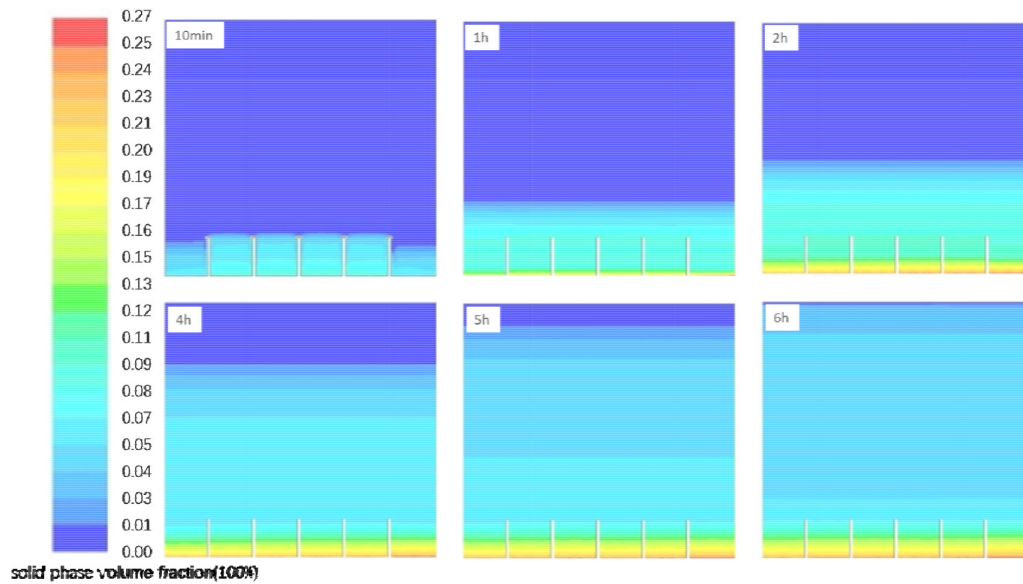


Fig. 13. The sand distribution during dynamic separation process at 50°C and 0.01 m/s inlet.

### 3.2.1.3. Comparison of sand velocity between 40°C and 50°C

By the comparison of sand velocity under two temperature conditions, as in Fig. 17, conclusions can be drawn as follows: ① The concentration distribution of liquid and solid phase is not obviously different under different temperature condition with the same injection flowrate when the time is less than 1 h. ② As the time is prolonged, the differences between the two

conditions emerge with respect to the velocity distribution. The height of solid phase at 40°C is higher than those at 50°C. This is because the velocity decreasing of sand is slower when sand moves upwards due to the larger drag force between sand and emulsion during the rising process when at 40°C. ③ By contrast, higher temperature and lower viscosity of emulsion are propitious to desand, but the influence is not obvious. Therefore, the desanding temperature can be 40°C when taking the energy cost for heating into consideration.

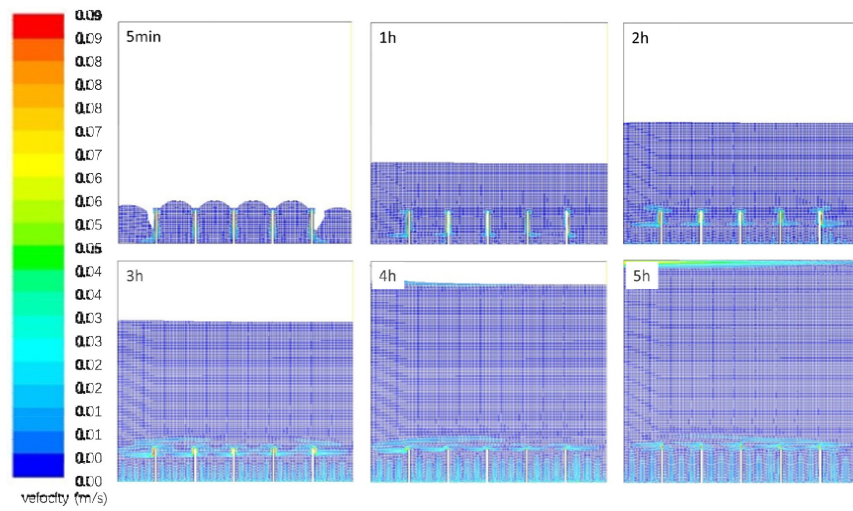


Fig. 14. The sand velocity distribution during dynamic separation process at 50°C and 0.01 m/s inlet.

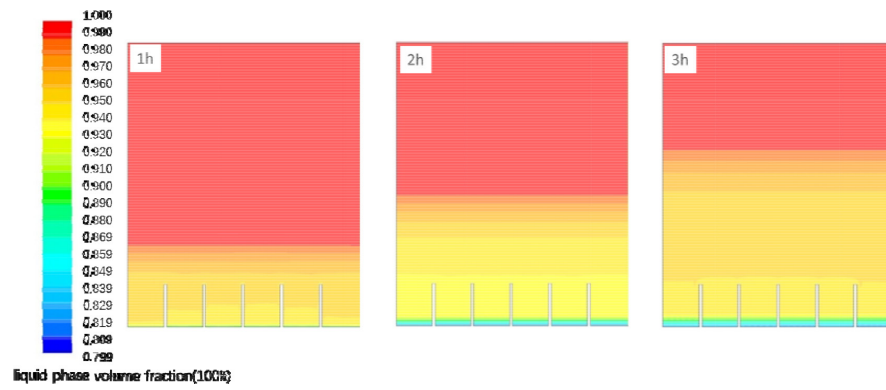


Fig. 15. The emulsion distribution during dynamic separation process at 40°C and 0.01 m/s inlet.

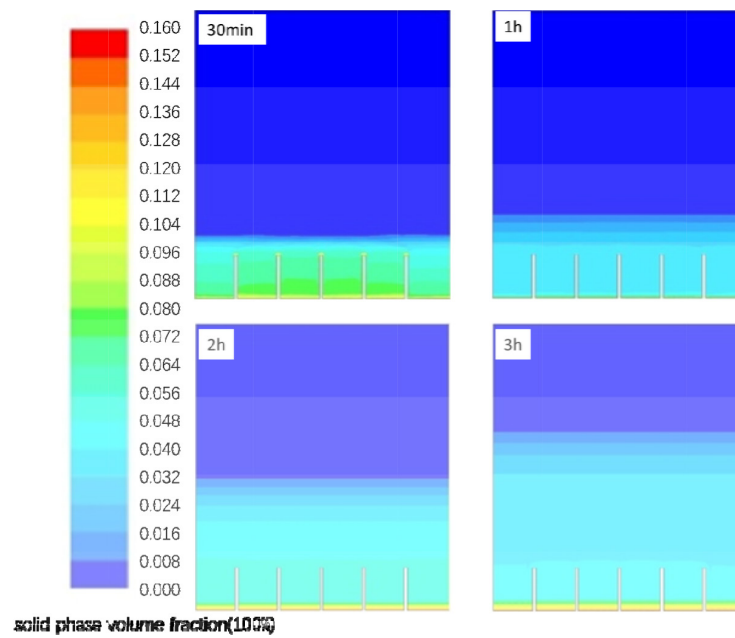


Fig. 16. The sand distribution during dynamic separation process at 40°C and 0.01 m/s inlet.

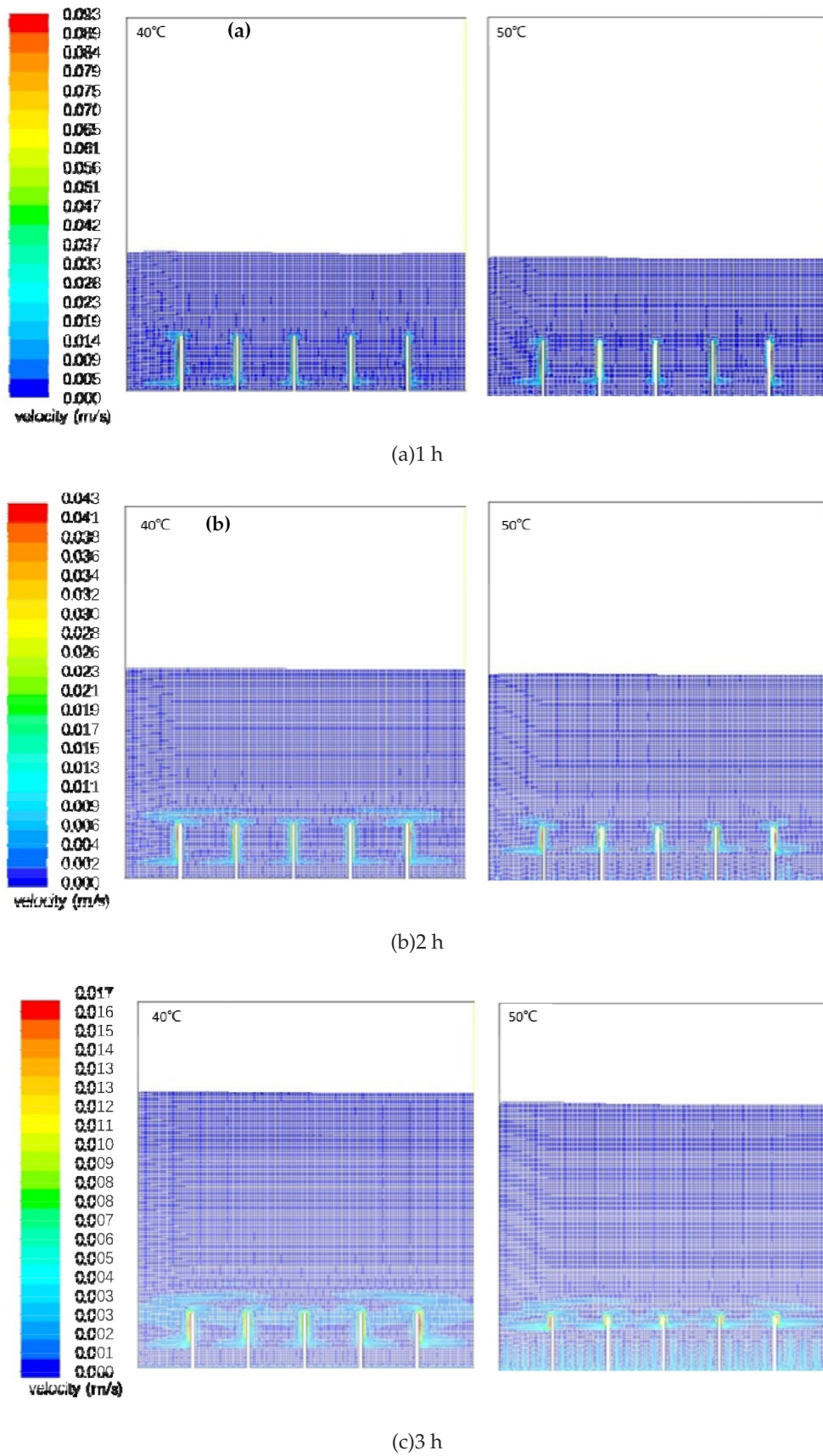


Fig. 17. The comparison of sand velocity at 40°C and 50°C, at an inlet speed of 0.01 m/s.

3.2.2 Effect of emulsion inlet speed on sand sedimentation

The distribution of emulsion is shown in Fig. 18 and the distribution of sand velocity is shown in Fig. 19, at 40°C and inlet speed of 0.05 m/s.

Figs. 18 and 19 show the distribution of liquid and solid phase during dynamic separation process with 40°C, at an inlet speed of 0.05 m/s, respectively. It can be found that the emulsion with over 4% of sand content has reached the top of the tank within 1 h. Due to the fast velocity, the sand has been effluent out of the tank without enough sedimentation time.

Fig. 20 shows the distribution of sand velocity. The emulsion has been effluent from the oil outlet at 40 min. The sand moves downward at the beginning, but turns upward apparently when the inlet speed becomes faster. The velocity inertia in the emulsion effluent leads the sand to move upward. Therefore, it can be concluded that the inlet speed of distributing pipe is limited by the capacity of the tank and the height of the distributing pipe. The better the desanding will be at the same inlet speed, with the larger tank capacity, the lower distributing pipe and the longer the emulsion stays at the tank.

Based on the analysis above, it can be concluded that the daily output of the big tank in high-sand-content oilfield can be calculated. Therefore, the volume of the sedimentation tank in high-sand-content oilfield without heating is given as:

$$V_{\text{tank}} = \frac{Q_{\text{total}}}{24 / \Delta t} = \frac{5400}{24 / 10} = 2250\text{m}^3 \quad (15)$$

Owing to the bigger emulsion viscosity in winter, 3000m<sup>3</sup> of sedimentation tank volume can be sufficient.

3.2.3. Effect of sand content on sand sedimentation

The influence of sand content on desanding between 5% and 20% of sand content is shown in this paper.

Fig. 21 illustrates the sedimentation process of desanding between 5% and 20% of sand content. By comparison, it can be found that the different sand content shows different sand settling velocity. That is, the less sand content will show faster sand sedimentation velocity. And when the sand accumulates at the bottom of the tank, the maximum of sand content is not 100% but 62.9%.

3.2.4. Effect of sand particle volume on sand sedimentation

According to the Stokes formula, when the sand continues to settle downward to the bottom of the tank, there will be pore space with the emulsion among the sand due to the spherical sand.

In the three-dimensional model (see Fig. 22), the ratio of sand volume to its corresponding tank volume is:

$$\frac{V_{\text{sand}}}{V_{\text{ideal}}} = \frac{\pi D_s^3}{D_s^3} = \frac{\pi}{6} \approx 0.523 \quad (16)$$

In the two-dimensional model, the ratio of sand area to the sectional area of the tank occupied by the sand is:

$$\frac{A_{\text{sand}}}{A_{\text{ideal}}} = \frac{\pi D_s^2}{D_s^2} = \frac{\pi}{4} \approx 0.785 \quad (17)$$

According to the simulation results, the sand content won't increase until the sand content at the bottom of the tank reaches 62.9%. The 62.9% is less than the ideal 2D ul-

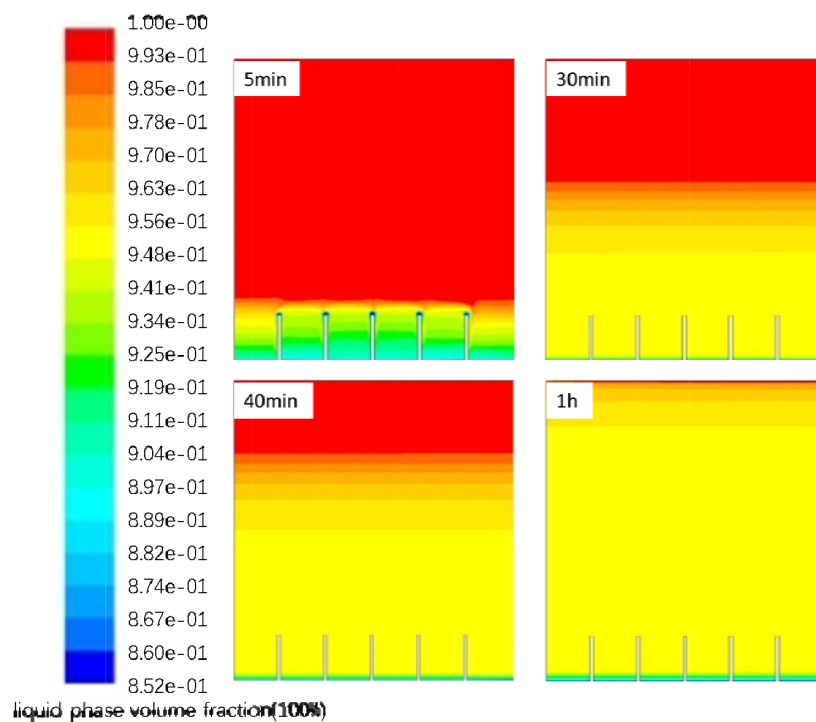


Fig. 18. The distribution of emulsion during dynamic separation process at 40°C, at an inlet speed of 0.05 m/s.

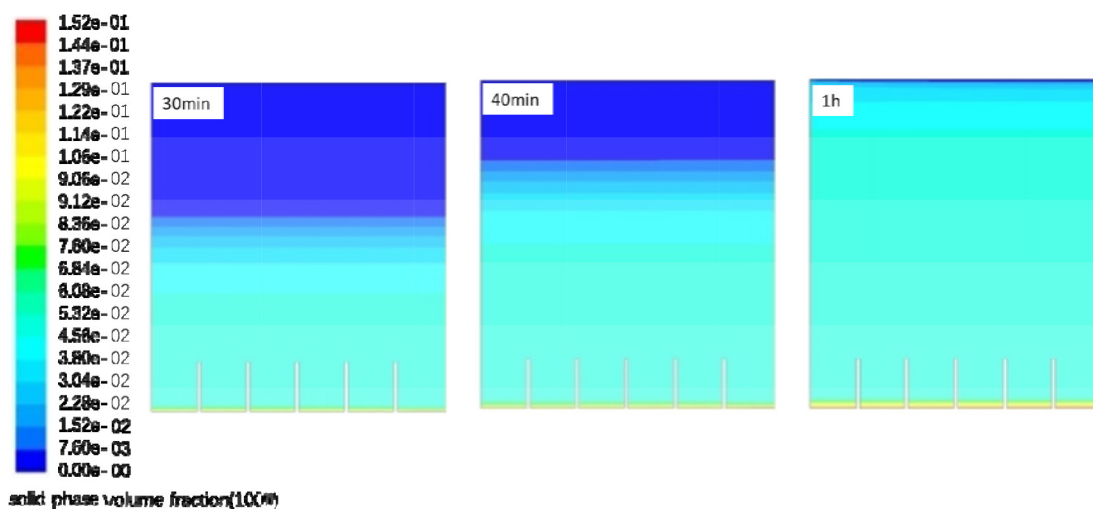


Fig. 19. The sand volume fraction during dynamic separation process at 40°C, at an inlet speed of 0.05 m/s.

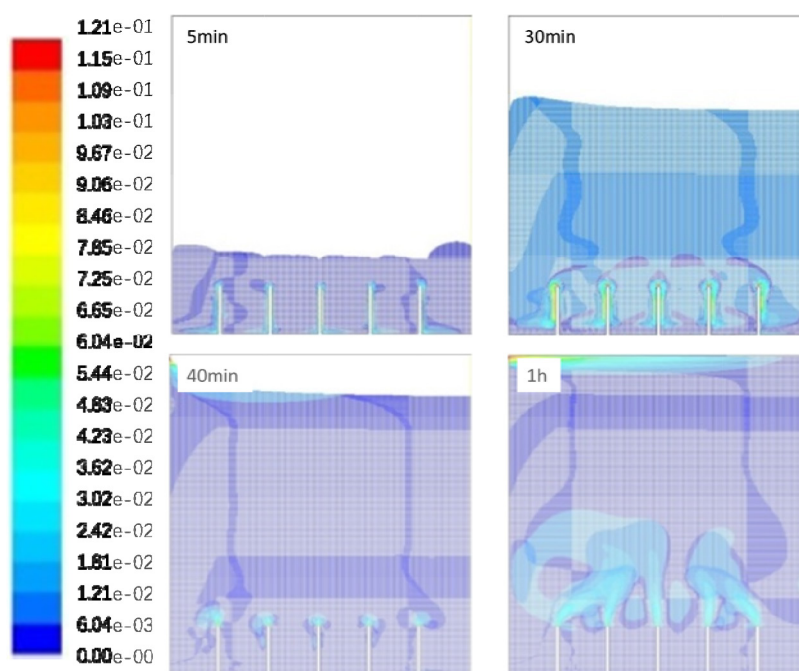


Fig. 20. The sand velocity during dynamic separation process at 40°C, at an inlet speed of 0.05 m/s.

mate sand content 78.5%, which means the sand doesn't deposit with an ideal state when considering the sand sedimentation in full flow field. Suppose that the maximum content of sand in sand sedimentation is  $f_{max}$ . According to the sand sedimentation, the highest sedimentation level  $h_{sand}$  at the biggest sand content should be lower than the height of the sedimentation tank  $h_{in}$ . Therefore, a time constraint on the sand cleaning periodic time  $T_1$  can be provided:

$$h_{sand} = \frac{Qf_oT_1}{\xi} \leq h_{in} \times f_{max} \Rightarrow T_1 \leq \frac{\xi \times h_{in} \times f_{max}}{Qf_o} \quad (18)$$

$$Qf_oT_2 \leq \xi \Rightarrow T_2 \leq \frac{\xi}{Qf_o} \quad (19)$$

Suppose that the volume of sand sedimentation at the tank bottom is  $\xi$  when the sand cleaning equipment arrives at its maximum capacity. Then the second constraint on sand cleaning periodic time can be provided as Eq. (20). Compared  $T_1$  to  $T_2$ , the minimal one is  $T_s$

$$T_s = \min(T_1, T_2) \quad (20)$$

### 3.3. Sand distribution in sedimentation tank

According to the simulation results under static and dynamic conditions, the distribution of solid phase is shown as follows:

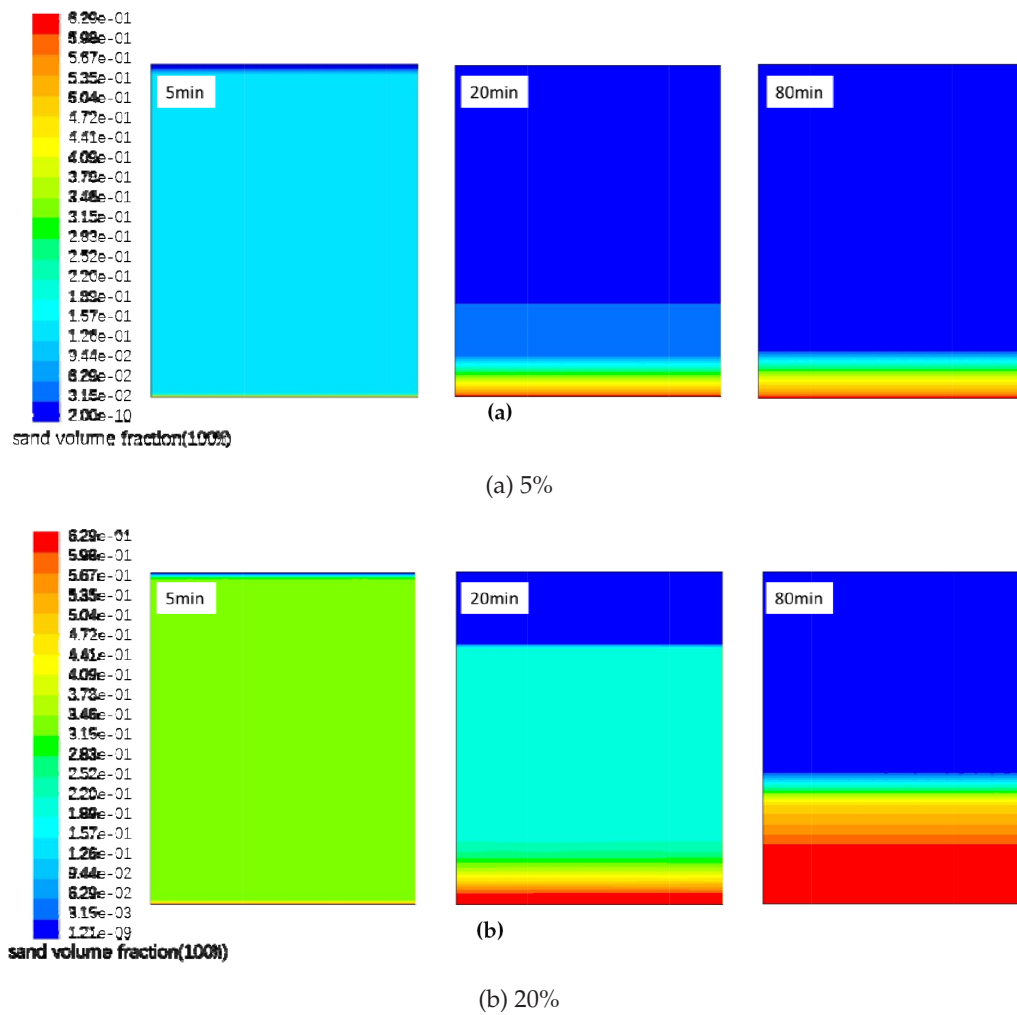


Fig. 21. The comparison of sand sedimentation between different sand contents.

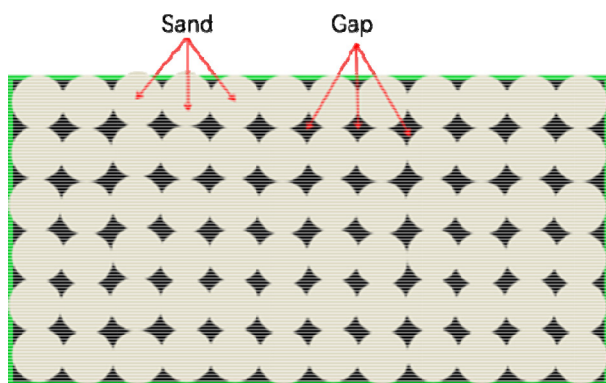


Fig. 22. The illustration of the space occupied by the sand and the pore space.

The sand content reaching effluent standard is  $f_o$ , the largest sand content at the bottom of the tank is  $f_{max}$ . Fig. 23 shows the illustration of distribution of solid phase with the sedimentation time (static state), and Fig. 24 shows the illustration of distribution of solid phase with injection (dynamic

condition). During static sedimentation process, the sand settles gradually due to the static condition. If the sand concentration at the tank bottom reaches the maximum  $f_{max}$ , the sand content won't increase, and the sand will stop sedimentation. If the sand content in emulsion located at the top of the tank is less than  $f_o$ , the effluent standard will be reached. This is the case that could be implemented in situ.

Comparatively, simulating the process of sedimentation under dynamic condition is more complex. The sand content near the distributing pipe reaches the highest level and the sand content near the height  $h_{in}$  at distributing pipe is equal to initial sand content in emulsion. The sand content gradually decreases at the area above the distributing pipe while it gradually increases below the distributing pipe. If the inlet speed of distributing pipe is faster than the safe speed of sand removal  $Q_o(v_o)$  leaving insufficient time for sedimentation, the emulsion will be effluent at the height of  $h_{out'}$ , however, at this time, the sand content doesn't meet the effluent standard, namely  $f > f_o$ . On the other hand, if the inlet speed of distributing pipe is slower than the safe speed of sand removal, the sand content will reach the effluent standard when the emulsion attaches the height of  $h_{out'}$ , namely  $f < f_o$ . This is the case that could be implemented in situ.

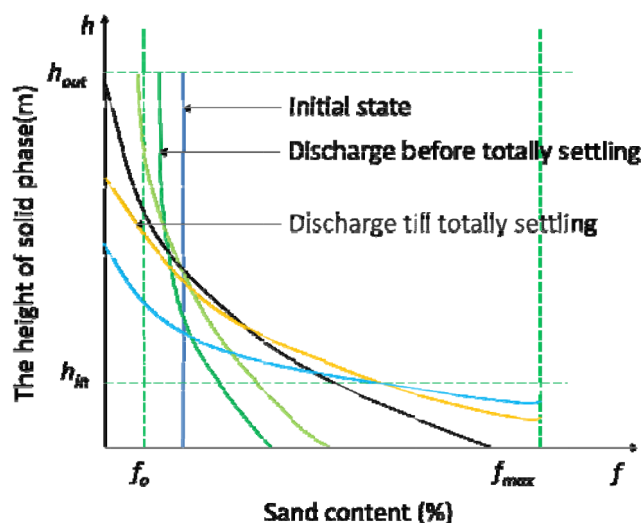


Fig. 23. The illustration of the distribution of the solid phase with sedimentation time (static condition).

During the simulation, the sand content decreased from 5% to 0.28% in 6 hours, and 0.1% in 10 h. Those data are obtained from Fig. 9. In the field experiment, settling tank used a volume of 3000 m<sup>3</sup> according to the simulation results. The sand content decreased from 5% to 0.08% in 10 h. In 15 h, the sand cannot be detected in the emulsion, which means the sand content is less than 0.05%. Comparison is shown as Fig. 25. Good agreement is achieved to prove the accuracy and effectiveness of the model.

### 3.4. Tracking of sand movement

The DPM model is used to simulate the trajectory of different sands with different sizes. The number of sand is 200. The diameter of spherical sand is 150  $\mu$ m, 120  $\mu$ m, 100  $\mu$ m, 90  $\mu$ m, 80  $\mu$ m, 70  $\mu$ m, 60  $\mu$ m, 50  $\mu$ m, 40  $\mu$ m, 30  $\mu$ m, 20  $\mu$ m and 10  $\mu$ m, and trajectory tracking is carried out respectively.

According to the boundary conditions of discrete phase, it is known that only the outlet and the inlet can be set as escape interfaces, and the others reflect interfaces. Because there is no escaping at the entrance, the escaping events only occur at the outlet. Therefore, the number of escaped sands is deemed to uselessness of separation, and other sands (deposited) are separated in the sand tank by sedimentation. Regardless of the strong effect among sand particles, the separation efficiency of each sand particle can be defined in Table 6.

It can be seen from Table 6 that the separation efficiency is becoming lower and lower as the diameter of sand decreases. The separation efficiency of sand is about 90% if its size is larger than 80  $\mu$ m. Through investigation, it is found that the sand with the size larger than 80  $\mu$ m can account for about 90% of the sand production in the oilfield, and the desanding efficiency of the sedimentation tank is about 90%. In addition, it is found that the sand with smaller size is easier to be brought to the downstream production facility by oil-water mixture.

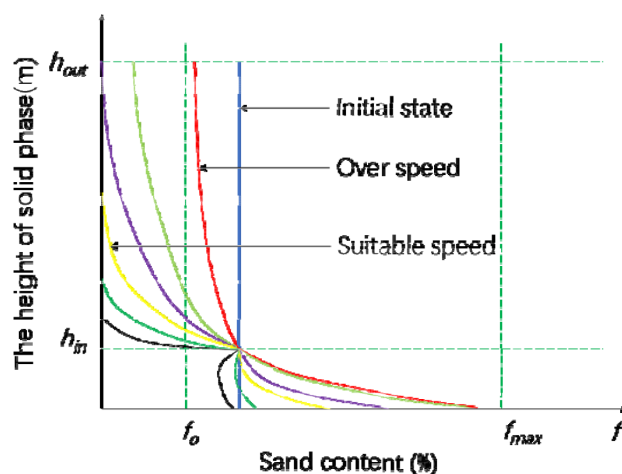


Fig. 24. The illustration of the distribution of the solid phase with sedimentation time (dynamic condition).

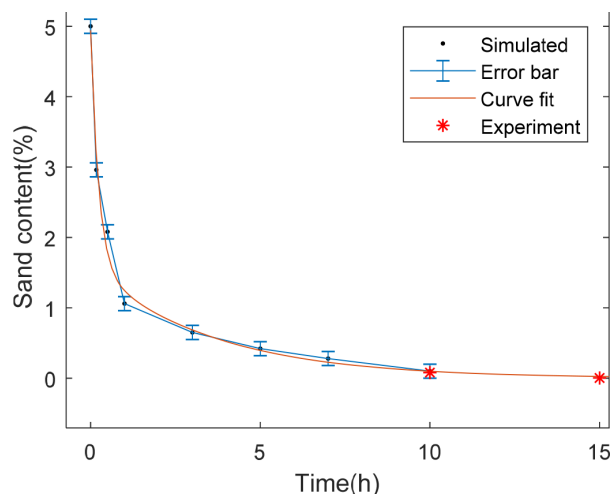


Fig. 25. Comparison between simulated results and experimental results.

Table 6  
The tracking results of sand with different diameters

Diameter ( $\mu$ m)	Quantity	Escaped	Deposited	Efficiency of separation (%)
150	200	0	200	100
120	200	3	197	98.5
100	200	5	195	97.5
90	200	10	190	95
80	200	20	180	90
70	200	42	158	79
60	200	60	140	70
50	200	90	110	55
40	200	116	84	42
30	200	140	60	30
20	200	176	24	12
10	200	196	4	2

Because the oil field production is continuous, if relevant measurements were not carried out in downstream for a long time, the production would be interrupted by sands with small diameter. Therefore, the oil producer should consider comprehensively whether to conduct the next sand removal means or not.

#### 4. Conclusion

According to the working principle of desanding in sedimentation tank, numerical method is adopted to simulate the internal flow field in the selected sedimentation tank. The separation efficiency of different sands with different sizes under different operating conditions were carried out. The main conclusions are as follows:

- (1) Compared with other models, the multiphase flow model Eulerian model and DPM model are chosen to simulate the depositing situation of water droplet and sand particle in the large size sedimentation tank. The calculation results show that the Eulerian model is suitable for the simulation of desanding in full flow field in sedimentation tank.
- (2) The sand sedimentation problem can be solved effectively in the sedimentation tank before entering the primary separator. At the same time, it can effectively improve the dehydration effect of separator. Under the same condition, a lower viscosity of the emulsion and a better desanding effect can be obtained if the sedimentation temperature of the tank is higher. The optimum sedimentation time is based on the amount of liquid in the coning pipe. The velocity constraint condition of the inlet of large tank is given, which provides reference for choosing sedimentation volume and optimizing sand removal process in sedimentation tank.
- (3) Through numerical simulation, the calculation formula of periodic time for cleaning large sedimentation tank is given in this paper, which provides references of cleaning frequency.
- (4) The separation efficiency of sands with different sizes can be measured by tracing the sand trajectory through using the DPM model. According to the analysis, the desanding efficiency can reach 90% when the sand size is larger than 80  $\mu\text{m}$ , which provides high-sand-content oilfield with reference that whether to add the next level of desanding equipment or not.
- (5) Combined with the simulation results in this paper and aiming at removing sands effectively, as well as reducing the energy consumption, it is suggested that the effluent-recycle should be abandoned and the sedimentation tank should be directly heated to reduce the viscosity of the liquid and prolong the sedimentation time, which is the optimum design for the whole desanding process.

#### Symbols

$A$	— The area of the two-dimensional cross section of the sedimentation tank ( $\text{m}^2$ )
$A_{ideal}$	— The area of corresponding square ( $\text{m}^2$ )
$A_{sand}$	— Round area of sand ( $\text{m}^2$ )
$D_s$	— Sand diameter (m)
$f^s$	— Volume fraction of sand in the tank, dimensionless
$f_{in}$	— The volume fraction of sand in the inlet emulsion, dimensionless
$f_{max}$	— The maximum volume of sand fraction at the bottom of the tank, dimensionless
$f_o$	— The volume fraction of sand in fluid that can reach the effluent standard, dimensionless
$h_{in}$	— Height of distributing pipe (m)
$h_{out}$	— Height of oil collecting pipe (m)
$h_{sand}$	— Height of sand deposition (m)
$L_{in}$	— Inlet length of distributing pipe (m)
$n$	— Number of distributing pipe inlets, dimensionless
$Q$	— The volume of liquid in the pipeline ( $\text{m}^3/\text{s}$ )
$Q_{total}$	— Total volume of liquid in the pipeline ( $\text{m}^3/\text{d}$ )
$Q_{in}$	— Injection flow of distributing pipe ( $\text{m}^3/\text{s}$ )
$t_1$	— Sedimentation time (s)
$T_1$	— Sand cleaning time frequency constrained by formula (18) (s)
$T_2$	— Sand cleaning time frequency constrained by formula (19) (s)
$T_s$	— Cleaning frequency (s)
$\Delta t$	— The time required for sand content in the emulsion that can reach the standard of outward effluent (h)
$v_{in}$	— The speed of liquid in an outlet pipe (m/s)
$V_{ideal}$	— The volume of corresponding cube ( $\text{m}^3$ )
$V_{sand}$	— The sphere volume of sand ( $\text{m}^3$ )
$V_{tank}$	— Volume of sedimentation tank ( $\text{m}^3$ )
$\zeta$	— The ratio of sand height $Qf_oT$ at the bottom of tank to the height $h_{sand}$ of sand deposition at the bottom of the tank, respectively the sand content in the sedimentation tank $f_o$ , and sand content at the oil collector $f_o$ , dimensionless
$\varsigma$	— The volume of bottom sand in the tank that can reach the upper limit of clearance capacity dimensionless

#### Acknowledgment

This work was supported by the National Natural Science Foundation of China [grant numbers 51474228].

#### References

- [1] E. Norval, R.H. Anderson, Design of final settling tanks for activated sludge, *Sewage Works J.*, 17(1) (1945) 50–65.
- [2] M.S.H. Bader, Sulfate scale problems in oil fields water injection operations, *Desalination*, 201(1) (2006) 100–105.
- [3] L.N. Chen, A fluent simulation of a vertical settling tank, Qingdao: China University of Petroleum (Hua Dong), (2010) 28–29.
- [4] D. Brennan, The numerical simulation of two phase flows in settling tanks, London: Imperial College London, 2001.
- [5] A. Deininger, E. Holthausen, P.A Wilderer, Velocity and solids distribution in circular secondary clarifiers: full scale measurements and numerical modelling, *Water Res.*, 32(10) (1998) 2951–2958.

- [6] K.Q. Dong, Study on closed sand cleaning device for crude settling tank, *J. Beijing Univ. Technol.*, 27(4) (2001) 476–478.
- [7] J.H.C. Roger, Particle characterization for oil sand processing 1: particle size measurements using a disc centrifuge, *Petrol. Sci. Technol.*, 17(3–4) (1999) 429–442.
- [8] W.T. Dong, Study on oil-water separation characteristics and structural optimization in settling tank, Daqing: Northeast Petroleum University, 2013.
- [9] D. Feng, S.Y. Li, C.J. Li, Present situation and development trend of ground sand removal equipment for sand production cold, *Petrol. Machinery*, 38(4) (2010) 65–68.
- [10] L. Fan, N. Xu, X. Ke, H. Shi, Numerical simulation of secondary sedimentation tank for urban wastewater, *J. Chin. I. Chem. E.*, 38(5) (2007) 425–433.
- [11] X. Liu, J. Li, Q. Zhu, J. Feng, Y. Li, J. Sun, The analysis and prediction of scale accumulation for water-injection pipelines in the daqing oilfield, *J. Petrol. Sci. Eng.*, 66(3) (2009) 161–164.
- [12] A.M. Goula, M. Kostoglou, T.D. Karapantsios, A.I. Zouboulis, The effect of influent temperature variations in a sedimentation tank for potable water treatment—a computational fluid dynamics study, *Water Res.*, 42(13) (2008) 3405.
- [13] A.M. Goula, M. Kostoglou, T.D. Karapantsios, A.I. Zouboulis, A CFD methodology for the design of sedimentation tanks in potable water treatment: case study: the influence of a feed flow control baffle, *Chem. Eng. J.*, 140(1) (2008) 110–121.
- [14] G.A. Hadi, J. Kriš, A numerical model of flow in sedimentation tanks in slovakia, *Pollack Periodica*, 3(2) (2008) 59–73.
- [15] H.L. Huang, Study on viscosity reduction and sand removal technology for heavy oil in Shuguang Oilfield, Hangzhou: Zhejiang University, (2015).
- [16] J. Kou, X.W. Cao, R.G. Xiao, Design and application of automatic desanding device for oil tank, *J. Xi'an Petrol. Univ.*, 22(3) (2007) 57–63.
- [17] P. Li, Study on removal of settling tank sludge by jet pump, Beijing: Beijing University of Chemical Technology, (2014).
- [18] E. Jassim, M.A. Abdi, Y. Muzychka, Computational fluid dynamics study for flow of natural gas through high-pressure supersonic nozzles: Part 2 Nozzle geometry and vorticity, *Petrol. Sci. Technol.*, 26(15) (2008) 1773–1785.
- [19] S.Y. Li, Z.W. Liu, W.Y. Liu, Automatic desanding technology for oil tank, *Petrol. Eng. Constr.*, 37(3) (2011) 58–60.
- [20] Z.Y. Shang, Q. Tang, Experimental study on automatic sand removal process for field oil collecting tank, *J. Yangtze Univ.*, 4(4) (2007) 111–113.
- [21] Y.B. Shao, Z.L. Nan, Z.J. Jin, Application of sand removal process in the transmission system, *Stand. Qual. Chin. PE. Ind.*, 23 (2013) 186–187.
- [22] G. Ahmadi, B. Firoozabadi, A. Tamayol, Determination of settling tanks performance using an eulerian-lagrangian method, *J. Appl. Fluid Mech.*, 1(1) (2008).
- [23] S.M. Tanin, Possibility of developing CFD web application to optimize sedimentation tank in WWTP, Norwegian: Norwegian University of Life Sciences, (2014).
- [24] R. Tarpagkou, A. Pantokratoras, CFD methodology for sedimentation tanks: the effect of secondary phase on fluid phase using DPM coupled calculations, *Appl. Math. Model.*, 37(5) (2013) 3478–3494.
- [25] H. Guo, S. J. Ki, S. Oh, Y.M. Kim, S. Wang, J.H. Kim, Numerical simulation of separation process for enhancing fine particle removal in tertiary sedimentation tank mounting adjustable baffle, *Chem. Eng. Sci.*, 158 (2017) 21–29.
- [26] M. Patziger, Computational fluid dynamics investigation of shallow circular secondary settling tanks: Inlet geometry and performance indicators, *Chem. Eng. Res. Des.*, 112 (2016) 122–131.
- [27] T. Bajcar, F. Steinman, B. Širok, T. Prešeren, Sedimentation efficiency of two continuously operating circular settling tanks with different inlet-and outlet arrangements, *Chem. Eng. J.*, 178 (2011) 217–224.
- [28] B. Xu, W. Kang, X. Wang, L. Meng, Influence of water content and temperature on stability of W/O crude oil emulsion, *Petrol. Sci. Technol.*, 31(10) (2013) 1099–1108.
- [29] P.F. Yao, Q.S. Zhang, R.G. Xiao, Automatic cleaning technology for settling sand of large tank in oilfield, *Cleaning World*, 29(12) (2013) 28–31.
- [30] W. Zhang, M. Chen, Technological design of automatic treatment equipment for oil sand tank of subsidence tank, *Oil Gas Field Surf. Eng.*, 22(2) (2003) 47–53.
- [31] L. Fan, N. Xu, X. Ke, H. Shi, Numerical simulation of secondary sedimentation tank for urban wastewater, *J. Chin. I. Chem. Eng.*, 38(5–6) (2007) 425–433.